# Terahertz Imaging Platform to Characterize the Growth of *In-Vitro* Breast Tumors

By: Scarlett-Marie Acklin
Department of Biological Sciences

Faculty Mentor: Dr. Magda El-Shenawee
Department of Electrical Engineering

## Abstract

This study aimed at evaluating the ideal plating method and density for imaging with the terahertz (THz) spectrometer. In this study, different methods were used to grow in-vitro tumors using the 4T1 cell line. Here, attempts to grow breast tumors in-vitro were conducted. Results were produced in two environments, flat-bottomed plates and round-bottomed multiwell plates. The second method allowed for faster clumping and increased cell aggregation, producing tumors up to 7mm. Terahertz spectroscopy produced images that correlated well to photomicrographs taken of the in-vitro tumors. This methodology shows great promise for providing a reliable, parameter-controlled source of in-vitro breast tumors for research needs on breast tumor margins.

## Introduction

Because breast cancer is the most common malignant disease in women (Weigelt et al., 2005), research to develop more effective treatments is extremely important. For the year 2015, the American Cancer Society predicts 234,190 new cases of breast cancer will be diagnosed and 40,730 deaths will occur (American Cancer Society, 2015). This statistic demonstrates an increase, rather than a decrease, in new cases of breast cancer from the year 2011. Routine screenings for breast cancer have become common practice in the United States since the 1960s, and x-ray mammography has been the primary method used (Hassan & El-Shenawee, 2011). The use of x-ray mammography comes with disadvantages; as a result, alternatives are being sought. For example, x-rays pose a health risk due to ionizing capabilities which are known to produce free radicals, break and form chemical bonds, and damage vital molecules such as deoxyribonucleic acid, ribonucleic acid, and proteins (Office of Environmental Health and Safety, 2015). This type of cell damage can lead to an increase in cancer development (Alberts et al., 2002), thereby compounding the problem. Additionally, the inaccuracy of x-ray mammography is high, ranging from 4% to 34% (Huynh et al., 1998). Magnetic resonance imaging (MRI) exists as an alternative to x-rays, but only for high-risk patients due to its expensive operating costs and its limited ability to distinguish between normal cells and cancerous cells, oftentimes leading to over-diagnosis (Hassan & El-Shenawee, 2011).

Removing the cancer before metastasis is also crucial, because metastases in the lymph nodes and other vital organs such as the lungs, liver, brain, and bones cause most of the complications linked to breast cancer, including death (Fantozzi & Christofori, 2006). During a lumpectomy to remove small tumors, a region surrounding the tumor, called the margin (Fig. 1) (Breastcancer.org, 2015) and (Bowman et al., 2015), is removed. A pathologist then examines the margin for cancerous cells. To maintain the best cosmetic appearance, it is important to differentiate between cancer, healthy fibrous and glandular tissue immediately surrounding the tumor, and healthy fatty breast tissue (Bowman et al., 2015). A positive margin, requiring a second surgery, demonstrates that cancer has extended across the edge of the excised tumor. The two other classifications do not require secondary surgery. The first of these is a close margin denoting cancer within 2mm of the tumor's edge and the second is a negative margin, where no cancer is detected within 2mm of the border. Positive margins not only cause cosmetic and emotional damage for the patient, but they are also very expensive due to the time and resources needed to carry out a second surgery. Research studies indicate that positive margins are detected 20-40% of the time (Pleijhuis et al., 2009).

A new medical imaging modality, available at the University of Arkansas, uses THz waves to develop high-resolution images and characterization of human breast tumors fixed in formalin and embedded in paraffin. THz waves measure from one mm to one μm, between infrared light and microwaves. Their

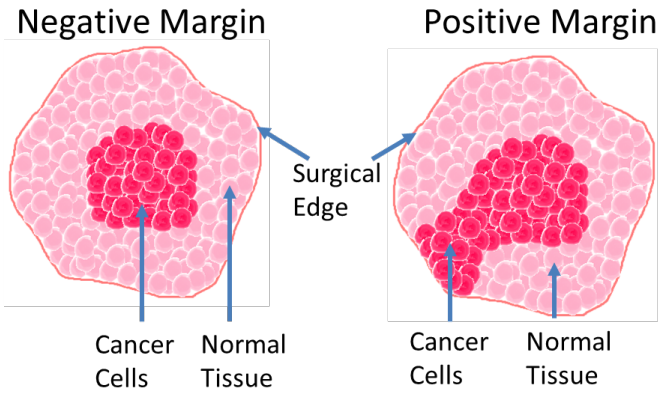


Figure 1. Animations of positive and negative margins (Breast Cancer Organization).

wavelengths have the medical advantage of possessing energy levels lower than the levels in x-rays that ionize cells (Burford et al., 2014). THz wavelengths have another advantage in that they are shorter than millimeter waves and therefore, generate higher image resolution while still penetrating the sample (Jepsen et al., 1996). Finally, THz waves produce limited levels of scattering in biological materials due to their longer wavelengths, instead of the strong scattering characteristic of near-infrared and visible wavelengths. Photons are scattered more strongly by biological materials because their size matches the incident wavelength (Wilmink & Grundt, 2011). For analysis, a THz pulse is emitted and strikes the sample, then a receiving antenna measures the intensity of the reflection off of the sample (Burford et al., 2014).

To further examine this new imaging system in a laboratory environment, attempts to grow breast tumors in-vitro were conducted. Current methods drip cells from an upper surface (Sato et al., 1977) or use multilevel chambers to pass the cells from an upper chamber, through a small pore, and into a bottom chamber where they are suspended from the roof (Dimri et al., 2007). The materials used in these methods are expensive and make the growth of multiple tumors unrealistic for most laboratories. Replacing these materials with agar gel and other commonly used substances could provide a reliable, parameter-controlled source of in-vitro tumors.

The cell line chosen for this experiment was the 4T1 mammary carcinoma cell line produced in BALB/cfC3H mice and first grown at the Karmanos Cancer Institute by Fred Miller (Tao et al., 2008). This cell line was chosen due to its tumorigenicity and invasivity. Furthermore, the 4T1 cell line is an ideal candidate for studying human breast cancer because metastasis occurs randomly from the initial tumor, the cells are transplantable so they can also be grown in *in vivo* environments, and its spread to the lymph nodes and other organs is similar to the metastasis in human breast cancer (Pulaski & Ostrand-Rosenberg, 2001).

## Methods and Materials

### 10% FBS DMEM media and 4T1 cell culture

A 10% FBS DMEM media was made from 50mL Fetal Bovine Serum, 5mL Penicillin-Streptomycin solution, 5mL L-glutamine, and 440mL Hyclone Dulbecco's High Glucose Modified Eagles Medium (DMEM). The 4T1 cell line was obtained from Dr. David Zaharoff's lab at the University of Arkansas. They were cultured in the 10% FBS DMEM media and incubated in a humidified environment at 37° C and washed with Phosphate Buffered Saline (PBS) every two-three days. Each week, the cells were passaged and two-three million cells were redistributed to a new flask with fresh media.

### Flat-bottomed plates

Each 60mm flat-bottomed culture plate was lined with 4mL of agar gel made from 2mL of 10% FBS DMEM media, 1.33mL of 1.8% Noble Agar, and .67mL of sterile water. After setting for ten minutes, a mix of 2.67mL of the 4T1 cell solution and 1.33mL of 1.8% Noble Agar was added on top of the gel. Once the gel set, 2mL of media was added on top and the plates were incubated for two nights. The plates were viewed under an optical microscope every two or three days for four weeks. Fresh media was added to the plates to provide a new nutrient source for the cells.

### Round-bottom multiwell plates

One percent agar was prepared from 40mL sterile water and .4g Difco Noble Agar, then autoclaved for fifteen minutes at 115°C to sterilize the solution. Fifty µL of agar was pipetted into each well of the first four rows (A-D) of a 96 well ultra-low attachment multiwell plate. The plate was constantly rotated as the gel cooled to ensure an even layer of gel coated the well while retaining the curved bottom surface. It was then overlaid with 10µL of 10% FBS DMEM media to

prevent the gel from drying out and allowed to incubate overnight. 150,000 cells were added to Row A, 300,000 were added to Row B, 600,000 were added to Row C, and 1.2 million were added to Row D. The 10% FBS DMEM media that contained the cells was changed every two to three days to continue providing nutrients.

**Preparation of the samples**

Multiple methods were used to prepare the samples for the THz spectroscopy and imaging system. Some of the flat-bottomed plates were fixed using a 2% paraformaldehyde solution while others were left as controls. Tissue Tek® O.C.T. Compound (OCT) was added to both samples in a plastic form to ensure optimal cutting temperature once frozen. Both types of plates were frozen and kept at -24°C. Using a Leica CM1860 cryostat, the samples were sectioned at a thickness of 20 µm.

The round-bottomed multiwell plate was frozen at -24° Celsius. Three samples with a starting cell count of 600,000 cells were sectioned with thicknesses of 40µm, 45µm, and 100µm and exposed to the air overnight to allow water molecules to evaporate from the OCT and gel before imaging. Another sample with a starting count of 1.2 million cells was sliced to a thickness of 40µm and placed directly on the viewing plate, preventing evaporation. A sample with a starting cell count of 150,000 cells was thawed, transferred directly to the viewing plate, and dried.

All samples were imaged using the TPS Spectra 3000 terahertz spectrometer from Teraview and analyzed using the TVL Imaging Suite (software package of the system).

## Results

**Flat-bottomed plates**

The spheroids grown in the flat-bottomed plates grew to a maximum size of 200 µm with a maximum center of 75 µm (Fig. 2). They were completely encased in the agar gel base and were easily sectioned due to the gel.

In order to obtain THz images, the spheroids were embedded in OCT compound. Imaging these samples using the THz system did not show any field significant reflection from the spheroid grown in flat-bottomed plates. As shown in Figure 3, the THz image

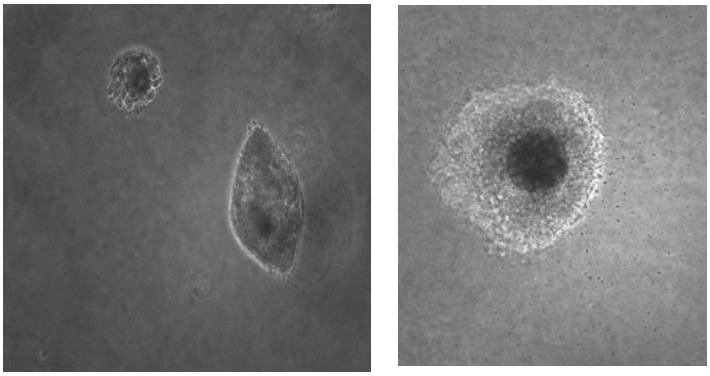

Figure 2. Photomicrographs of spheroids from flat-bottomed plates. Spheroids were immersed within the gel and imaged at 4× magnification.

demonstrates almost uniform reflection off the entire surface of the sample. The reflection imaging module of the THz system is shown in Figure 4.

**Round-bottom multiwell plates**

Wells containing over 150,000 cells appeared crowded with no areas of increased cell concentration or spheroid formation. The samples obtained from the 600,000 wells were difficult to section and the gel appeared very brittle and fragmented. Upon slicing, the gel containing the sample would flake and disintegrate as it rolled off the sample block or came into contact with the metal on the cryostat machine. Thicker sections were taken to obtain a solid sample without flaking. THz viewing showed no positive reflection where the tumor should have been. The 40µm slice showed the same reflection in the center of the OCT, where the tumor should have been, as the

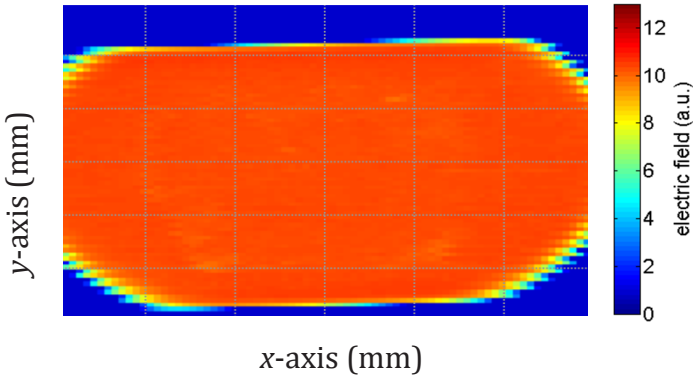


Figure 3. Cross section of 4T1 spheroids from flat-bottomed plate. The sample was embedded in agar gel and OCT compound. A 20µm thick section was cut and imaged using the THz spectroscopy and imaging system.

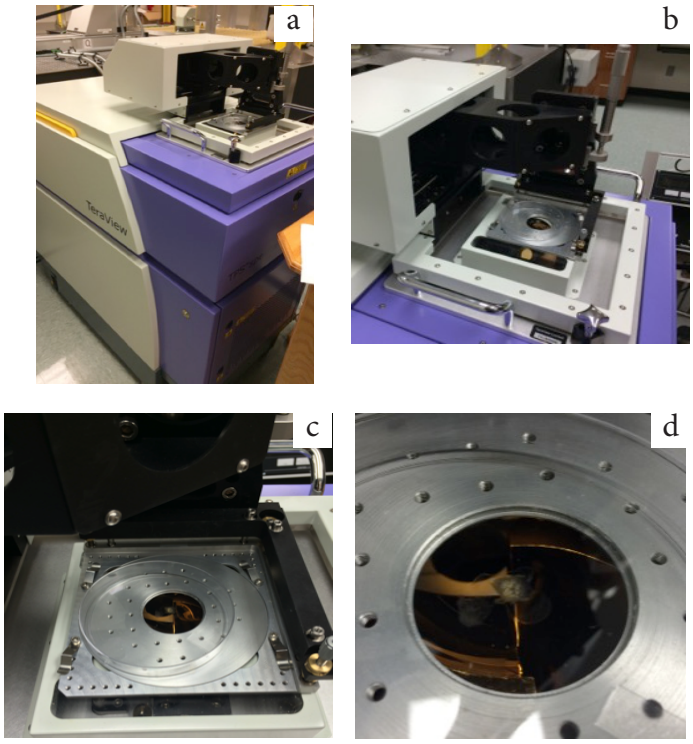


Figure 4. Images of the TPS Spectra 3000 spectrometer a) shows the core system as a whole, b) shows more detail of the reflection imaging module, c) shows the placement of samples within the viewing window, and d) shows a close-up of a potential sample.

area that had only the viewing plate (Fig. 5). The same was the case for the 45µm (Fig.6) and 100µm (Fig. 7) slices. The bright blue spot on the 100µm slice was observed as a bubble (Fig. 7).

The sample from the well, beginning with 1.2 million cells, again disintegrated during sectioning and only showed a single reflection off the center of the viewing plate. No spheroids or concentrations of cells were present (Fig. 8).

Wells with 150,000 starting cells produced spheroids centered in the middle with multiple tighter spheroids around the edges (Fig. 9). Transportation of the samples to the viewing plates showed the tumors were embedded into the gel, but it is not clear how deep.

The colors seen on the THz images are assigned arbitrarily to best show the difference in reflections that are given off because the original image is black and white. THz spectroscopy showed a difference in reflection between the media that contained the sample and the tumors as a whole. In Figure 10a, the medium blue area surrounding the brighter blue shows a negative reflection, but one with a lower magnitude than the viewing plate. The brightest blue shows a positive reflection while the darkest blue shows a negative

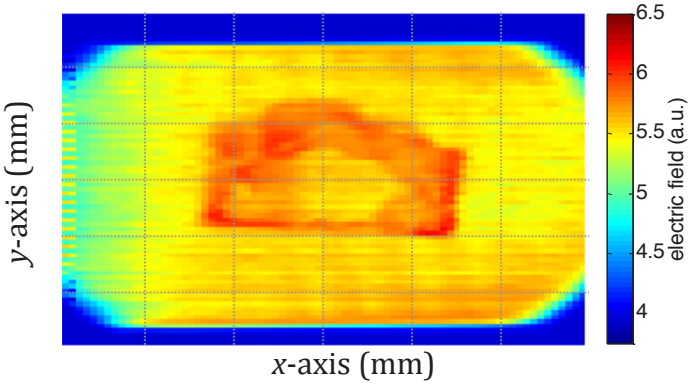


Figure 5. Cross section of 4T1 spheroid from 600,000 starting cells. The sample was embedded in agar gel and surrounded by OCT Compound. A 40 µm thick section was cut and imaged using the THz spectroscopy and imaging system. The yellow area, where the tumor should have been, within the red are indicates a lack of cancer cells.

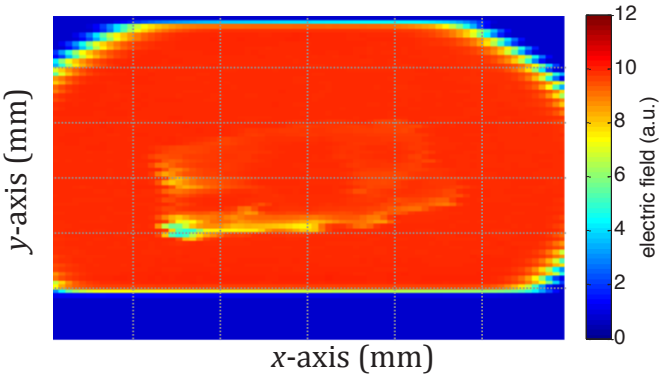


Figure 6. Cross section of 4T1 spheroid from 600,000 starting cells. The sample was embedded in agar gel and surrounded by OCT Compound. A 45µm thick section was cut and imaged using the THz spectroscopy and imaging system. The uniform reflectance across the sample indicates a lack of cancer cells.

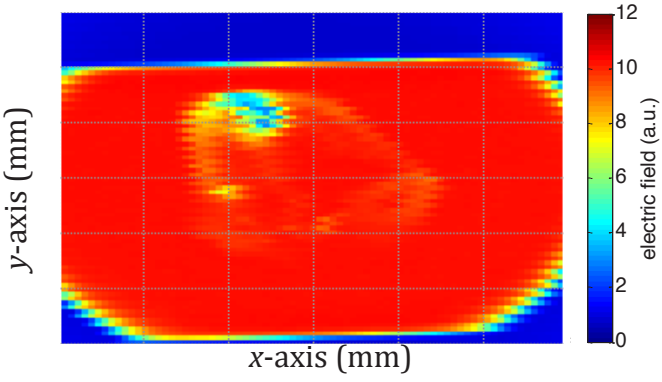


Figure 7. Cross section of 4T1 spheroid from 600,000 starting cells. The sample was embedded in agar gel and surrounded by OCT Compound. A 100µm thick section was cut and imaged using the THz spectroscopy and imaging system. The uniform reflectance across the sample indicates a lack of cancer cells, as the blue portion was a bubble.

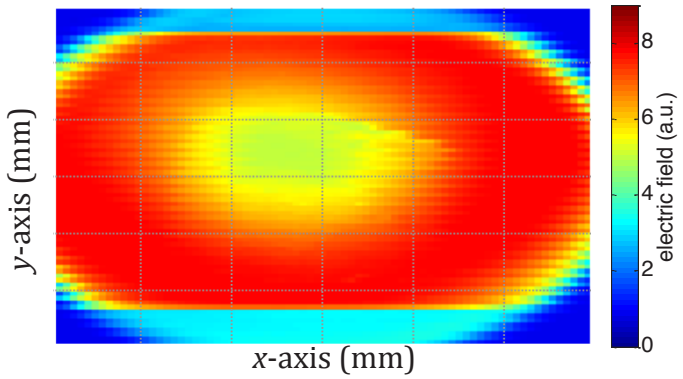


Figure 8. Cross section of 4T1 spheroid from 1,200,000 starting cells. The sample was embedded in agar gel and surrounded by OCT Compound. A 40 thick section was cut and imaged using the THz spectroscopy imaging system. The single reflectance in the center of the image corresponds to only OCT compound and indicates a lack of a tumor.

reflection. The area of positive reflection corresponded to the area of high cell density on the microphotograph and the negative reflection responded to the area of low density. The tumor measured about 5mm in diameter.

Figure 11a shows similar results with the central

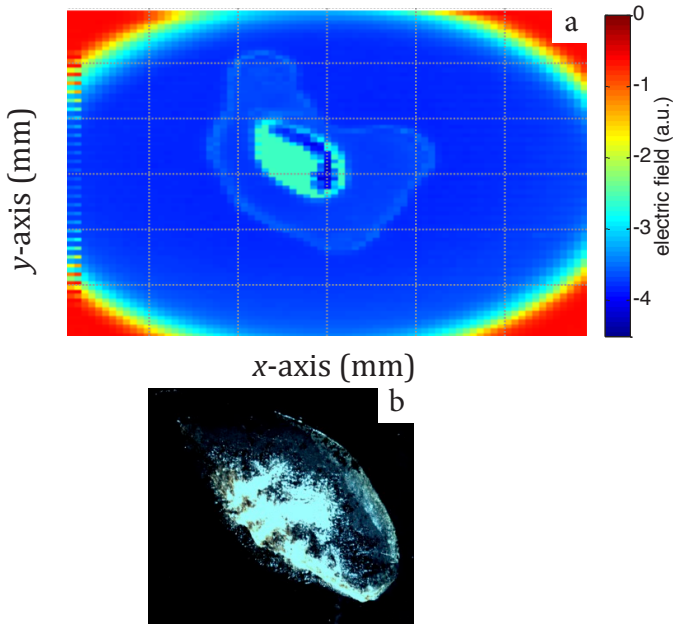


Figure 10. THz cross sections of 4T1 spheroids from 150,000 starting cells, first sample. The sample was embedded in agar gel and processed in its entirety using the THz spectrometer and imaged at 4× magnification. Figure a, shows positive reflection in the bright blue area and negative reflection in the darkest blue area, corresponding to the area of highest density and area of low density in the microphotograph shown in Figure b. The image was taken of the entire sample in a petri dish.

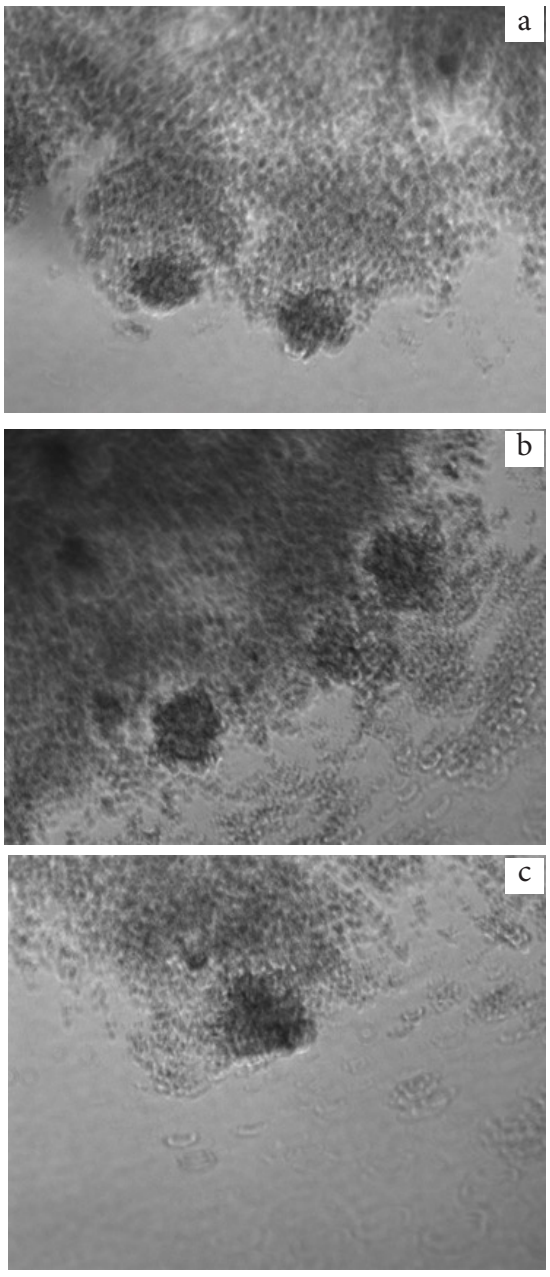


Figure 9. Photomicrographs of spheroids at 10× magnification from round-bottomed multiwell plate. The cells and spheroids were embedded into the gel base layer and the initial cell count was 150,000. Figures a, b, and c represent the spheroids clusters taken at different position of the sample.

red area exhibiting a positive reflection, the darkest blue area showing a negative reflection, and the yellow area around it demonstrating a negative reflection with a lower magnitude than the viewing plate. The red area correlated to the area of high density on the microphotograph and the dark blue correlated to the area of low density. Approximate size of the tumor was 7mm in diameter.

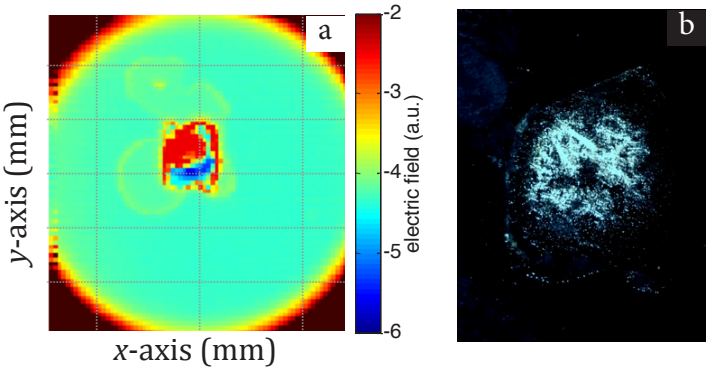


Figure 11. THz cross sections of 4T1 spheroids from 150,000 starting cells, second sample. The sample was embedded in agar gel and processed in its entirety using the THz spectrometer and imaged at 4× magnification. Figure a, shows positive reflection in the red area and negative reflection in the darkest blue area, corresponding to the area of highest density and area of low density in the microphotograph shown in Figure b. The image was taken of the entire sample in a petri dish.

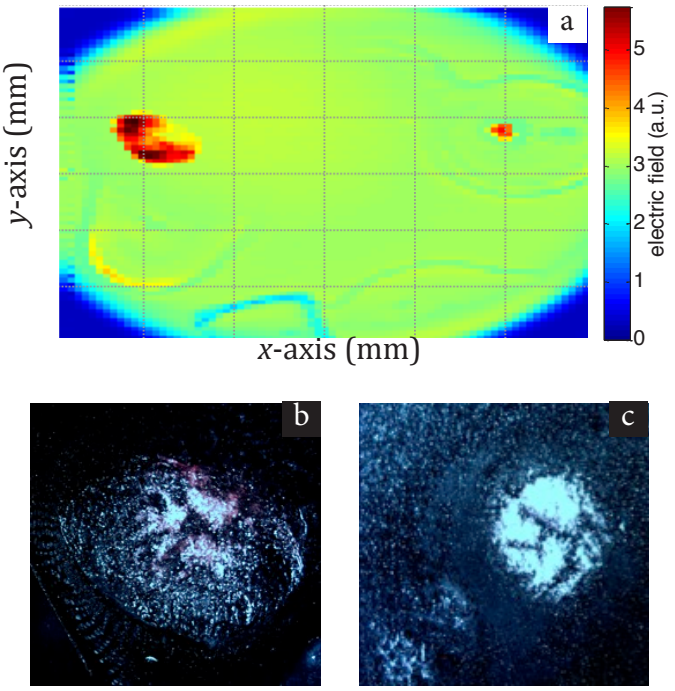


Figure 12. THz cross sections of 4T1 spheroids from 150,000 starting cells, third sample. The sample was embedded in agar gel and processed in its entirety using the THz spectrometer and imaged at 4× magnification. Figure a, shows positive reflection in the red areas and even stronger positive reflection in the black areas, corresponding to the multiple areas of thick cell density area in the microphotograph shown in Figures b and c. The image was taken of the entire sample in a petri dish.

Figure 12a also supported the previous findings. The red and black areas showed positive reflection, with black having a higher magnitude. The two black areas in the larger spheroid corresponded to the split spheroid seen in Figure 12b, although the orientation did not completely correspond. The second, smaller tumor was also seen in the microphotograph and measured 2mm in diameter while the larger one measured 5mm in diameter.

All THz images presented in this work represent the peak of the electric field reflected from the samples expressed in arbitrary units (a.u.), which could be the positive peak or the negative peak of the pulse.

## Discussion

Using the round-bottom multiwell plate helped aggregate the 4T1 cells together and gave them greater opportunities for cell-to-cell contact to form the primary tumor as well as the peripheral spheroids. The sample obtained from the round-bottomed well was 25×the size of the largest spheroid grown in the flat-bottomed plates. However, the environment in the flat-bottomed plate ensured the tumor was fully encased in gel, as it would be in an actual patient. Growing in this environment is not an option for this project, though, because the THz spectroscopy was not able to produce results from the sample. The insignificant reflection of the electric field shown on the THz image is likely due to the spheroids being too small for viewing, or the section could have been too thin leading to desiccation and loss of sample.

In the round-bottom environment, the uniform dispersal of cells starting with more than 150,000 cells suggests there is an upper limit to the cell count that can grow in a multiwell plate of this size. Potential causes are lack of space, lower nutrient:cell ratio, and limited access to the nutrients contained in the media. In order to remove the entire sample from the well and ensure all parts of the tumor were removed as a whole; freezing initially seemed to be the best option because it is also required for sectioning. However, the agar gel became too brittle at the -24°C temperature in which it is sectioned, and prevented a quality sample of the actual tumor from being included with the OCT Compound in the sample slice. This is shown in Figures 5-7 where the OCT produced electric field reflection different from that of the viewing plate, but the center of the plate had the same reflection as the plate. Additional samples were placed onto different material, polyurethane, to

ensure this was not the result of the sample having a refractive index equal to that of the original glass slide. Figure 8 also supports the concept that the wells cannot hold that many cells as it produces a uniform electric field reflection across the entire slide.

Transferring the sample directly to the viewing plate corrected this problem while still differentiating between the media and the 4T1 cells and eliminated the need for the OCT compound. The resolution of the THz system was not able to distinguish between the entire sample and the tighter spheroids that were attached to the outer edge of the tumor. This would be of less significance when dealing with a patient with breast cancer because the tumor would be a size large enough to be detected using the THz system.

Microphotographs of the spheroids from the 150,000 wells strengthen the findings of the THz imaging. Figure 10b aligns with 10a and shows a higher cell concentration and tumor height on the left of the image. More cells are seen on the right, with a much lower density in between. Figures 11a and 11b also correspond to each other, showing decreased tumor thickness on the bottom left corner of the sample. Finally, Figures 12b and 12c illustrate the results obtained in 12a. The microphotograph reveals the two dark areas within the tumor as areas of greater tumor thickness and gives more detail to the smaller, separated spheroid.

Based on the results, particularly Figure 12c that shows a separate smaller spheroid that grew in addition to the primary tumor, THz imaging and spectroscopy is a viable method for detecting breast cancer tissues of patients with tumors 2mm or larger. This size is much lower than the current median detectable size, 7.5mm (Michaelson et al., 2003). For future research, it is recommended plating 150,000 4T1 cells in a 96 well multiwell plate with a base layer of agar maintaining the rounded shape. To prepare and image the sample using the THz spectrometer, the sample should be transferred directly to the viewing plate without prior freezing and all water should be evaporated overnight.

The initial goal of this project was to grow breast tumors in vitro that mimic in vivo tumors in size and encasement in a flexible substance. While the tumors were limited in size, the results revealed a new methodology for growing tumors for THz spectroscopy at a lower cost that could be replicated on a larger scale.

Works Cited

1. Alberts, B., Johnson, A., Lewis, J., Raff, M., Roberts, K., & Walter, P. (2002). *Molecular Biology of the Cell*. New York. Garland Science.
2. American Cancer Society (2015). "Cancer Fact & Figures". American Cancer Society. http://www.cancer.org/ March 2015.
3. Bowman, T. C., El-Shenawee, M., & Campbell, L. K. (2015). Experimental terahertz z-scan imaging of three-dimensional paraffin embedded breast cancer tissue. *Proceedings of IEEE MTT-S International Microwave Symposium*, Phoenix, AZ, USA.
4. Bowman, T. C., El-Shenawee, M. & Campbell, L. K. (2015). Terahertz imaging of excised breast tumor tissue on paraffin sections. *IEEE Transactions on Antennas and Propagation*, 63, 2088-2097.
5. Breastcancer.org (2015), "Surgical Margins". http://www.breastcancer.org/ March 2015.
6. Burford, N., El-Shenawee, M, O'Neal, C.B. & Olejniczak, K. J. (2014). Terahertz imaging for nondestructive evaluation of packaged power electronic devices. *International Journal of Emerging Technology and Advanced Engineering*, 4, 395-401.
7. Dimri, M., Naramura, M., Duan, L., Chen, J., Ortega-Cava, C., Chen, G., Goswami, R., Fernandes, N., Gao, Q., Dimri, G. P. Band, V., & Band, H. (2007). Modeling breast cancer-associated c-Src and EGFR overexpression in human MECS: c-Src and EGFR cooperatively promote aberrant three-dimensional acinar structure and invasive behavior. *Cancer Research*, 67, 4164-4172.
8. Fantozzi, A. & Gerhard, C. (2006). Mouse models of breast cancer metastasis. *Breast Cancer Research*, 8, 212.
9. Hassan, A. M., and El-Shenawee, M. (2011). Electromagnetic techniques for breast cancer detection. *IEEE Reviews in Biomedical Engineering*, 4, 103-118.
10. Huynh, P., Jarolimek, A., & Susanne, D. The false-negative mammogram. (1998). *RadioGraphics*, 18, 1137–1154.

11. Jepsen, P., Jacobsen, R., & Keiding, S. (1996). Generation and detection of terahertz pulses from biased semiconductor antennas. *Journal of the Optical Society of America B*, 13, 2424-2426.
12. Michaelson, J., Satija, S., Moore, R., Weber, G., Halpern, E., Garland, A., Kopans, D. B. & Hughes, K. (2003). Estimates of the sizes at which breast cancers become detectable on mammographic and clinical grounds. *Journal of Women's Imaging*, 5, 3-10.
13. Office of Environmental Health and Safety. (2015). Biological effects of ionizing radiation. *Princeton University*. 9 Apr. 2014. Web. 29 Mar. 2015.
14. Pleijhuis, R. G., Graafland, M., de Vries, J., Bart, J., de Jong, J. S., van Dam, G. M. (2009). Obtaining adequate surgical margins in breast conserving therapy for patients with early-stage breast cancer: Current modalities and future directions. *Ann. Surg. Oncol*., 16, 2717–2730.
15. Pulaski, B., & Ostrand-Rosenberg, S. (2001). Mouse 4T1 breast tumor model. *Current Protocols in Immunology*, 39, 20.2–20.2.16.
16. Sato, H., Goto, M., & Shigetoshi, H. (1977). Growth behavior of ascites tumor cells in three-dimensional agar culture. *Tohoku Journal of Experimental Medicine*, 122, 155-160.
17. Tao, K., Fang, M., Alroy, J. & Sahagian, G. G. (2008). Imagable 4T1 model for the study of late stage breast cancer. *BMC Cancer*, 8, 228. .
18. Weigelt, B., Peterse, J., & Laura, J.V. (2005). Breast cancer metastasis: markers and models. *Nature Reviews*, 5, 591-602.
19. Wilmink, G., & Grundt, J. (2011). Current state of research on biological effects of terahertz radiation. *Journal of Infrared, Millimeter and Terahertz Waves*, 32, 1074-1122.